

Evaluation of the minimum iodine concentration for contrast enhanced subtraction mammography

P. Baldelli^{a,*}, A. Bravin^b, C. Di Maggio^c, G. Gennaro^c, M. Gambaccini^a,
A. Sarnelli^a, A. Taibi^a

^aPhysics Department, University of Ferrara and INFN Section of Ferrara, Italy

^bEuropean Synchrotron Radiation Facility, Grenoble, France

^cDepartment of Oncological and Surgical Sciences of Padua, Italy

Available online 12 July 2007

Abstract

The aim of this work is to investigate the use of iodine based contrast media in mammography with two different double exposure techniques: K-Edge Subtraction Mammography and Temporal Subtraction Mammography. Both techniques have been investigated by using monochromatic beams produced at a synchrotron radiation facility and conventional beams obtained with a clinical digital mammography system. A dedicated three-component phantom containing cavities filled with different iodine concentrations has been developed and used for measurements. For each technique, information about the minimum iodine concentration which provides a significant enhancement of the detectability of the pathology by minimizing the risk due to high dose and high concentration of contrast medium has been obtained. In particular for cavities of 5 and 8 mm of diameter filled with iodine solutions (0, 2, 4, 8, 16, 32 mg/ml), the minimum concentrations needed to obtain a contrast-to-noise ratio of 5 with a mean glandular dose of 2 mGy have been obtained. © 2007 Elsevier B.V. All rights reserved.

PACS: 87.59.-e; 87.59.Ek

Keywords: Dual-energy; Mammography; Contrast medium

1. Introduction

In mammography, 10–20% of breast cancers [1], including at least 9% of the ones already palpable, are not depicted. In fact, early manifestation of breast cancer is often very subtle and is displayed in a complex and variable pattern of normal anatomy that may obscure the disease. This is particularly important in dense breasts, found in approximately 25% of the women, caused by the complexity of overlying fibroglandular structures. Dual-energy mammography with contrast medium could help to enhance the detectability of lesions by removing the structure noise and enhancing the region surrounding the tumour. The aim of this work is to investigate the use of contrast media in mammography with two different double exposure techniques: K-Edge Subtraction Mammography (KESM) and Temporal Subtraction Mammography (TSM).

These techniques have been investigated by using synchrotron radiation and a digital conventional system.

A dedicated three-components phantom containing details of two different sizes filled with various concentrations of iodine has been developed.

The parameter CNR^2/MGD (contrast-to-noise ratio)²/(Mean Glandular dose) has been used as a figure of merit to compare the two techniques. In particular the minimum contrast medium concentration needed to visualize a detail with an $CNR = 5$ and an $MGD = 2$ mGy, has been achieved.

2. Equipment and method

2.1. The three component phantom

A three-component breast phantom was specifically built to perform dual-energy analysis. The phantom consists of a 5 cm thick polymethylmethacrylate (PMMA) box, filled with animal fat for simulating adipose tissue and PMMA spheres of two

*Corresponding author. Tel.: +39 0532 974218.
E-mail address: baldelli@fe.infn.it (P. Baldelli).

different diameters, 8 and 12.7 mm, respectively, for simulating fibroglandular tissue. The use of spheres makes the phantom non-uniform like the variable pattern of normal anatomy of the breast. A 1 cm thick PMMA slab containing cavities with two different diameters (5 and 8 mm) is placed in the middle of the box (see Fig. 1). Cavities have been filled with different solutions of water and Ultravist (iopromide, 370 mg/ml iodine, Berlex Laboratories, Montville, NJ), corresponding to iodine concentrations of 0, 2, 3.98, 8, 16.1 and 33.6 mg/ml.

2.2. Mathematical formalism of the dual-exposure algorithm

With the K-edge subtraction technique two images, acquired at different energies after the contrast medium administration, are subtracted to highlight structures uptaking contrast medium. This technique takes advantage of the sharp rise of the absorption coefficient of a suitable contrast agent, thus performing the acquisition of two images after the injection of the contrast agent at energies just below and above the K-edge energy. By using the Lehman's algorithm it is possible to decompose the phantom in two base materials [2] (iodine and water in this work) and to obtain two final images: the *iodine* image that is a map of the iodine distribution and the *water* image that is the map of all other materials. They are given by

$$(\rho t)_I = \frac{\left[\frac{\mu}{\rho}(E_-) \right]_w \ln \frac{N_0}{N}(E_+) - \left[\frac{\mu}{\rho}(E_+) \right]_w \ln \frac{N_0}{N}(E_-)}{K_0}, \quad (1)$$

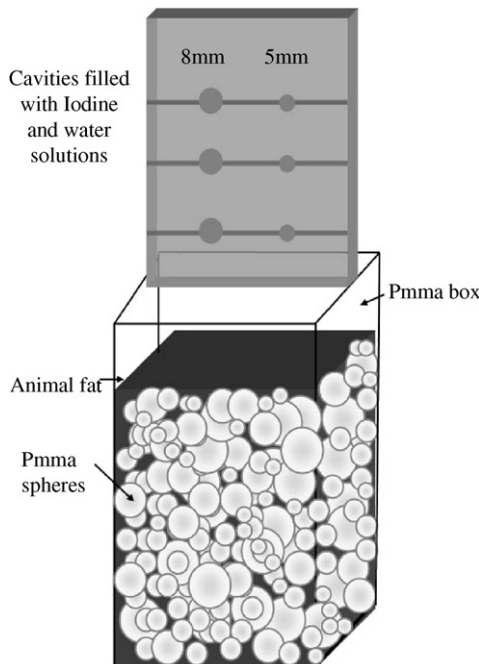


Fig. 1. Scheme of the three component phantom developed for dual energy application.

$$(\rho t)_w = \frac{\left[\frac{\mu}{\rho}(E_+) \right]_I \ln \frac{N_0}{N}(E_-) - \left[\frac{\mu}{\rho}(E_-) \right]_I \ln \frac{N_0}{N}(E_+)}{K_0}, \quad (2)$$

with

$$K_0 = \left[\frac{\mu}{\rho}(E_-) \right]_w \cdot \left[\frac{\mu}{\rho}(E_+) \right]_I \left[\frac{\mu}{\rho}(E_+) \right]_w \cdot \left[\frac{\mu}{\rho}(E_-) \right]_I, \quad (3)$$

where N_0 is the mean number of incident photons per area unit, N is the number of photons impinging on the detector after the transmission through the object, E_+ and E_- are the two energies that bracket the K-edge discontinuity, $(\mu/\rho)_I$ and $(\mu/\rho)_w$ are mass attenuation coefficients of iodine and water at the energies of interest, $(\rho t)_I$ is the mass density of iodine and $(\rho t)_w$ is the water equivalent mass density of all other materials.

The second technique applied is the TSM [3] which is based on the acquisition of two images at the same energy: an initial *mask* image, followed by an image obtained after contrast agent administration. Following image registration, the logarithm of the mask image is subtracted from the logarithm of the post-contrast image.

2.3. Image acquisition

2.3.1. Acquisition of images with monochromatic X-rays

X-ray imaging experiments with a monochromatic source have been carried out at the ID17 biomedical beamline of the European Synchrotron Radiation Facility (ESRF) [5]. The detector used is a high-purity germanium detector (HPGe) operating at liquid nitrogen temperature. For the KESM technique application, images of the

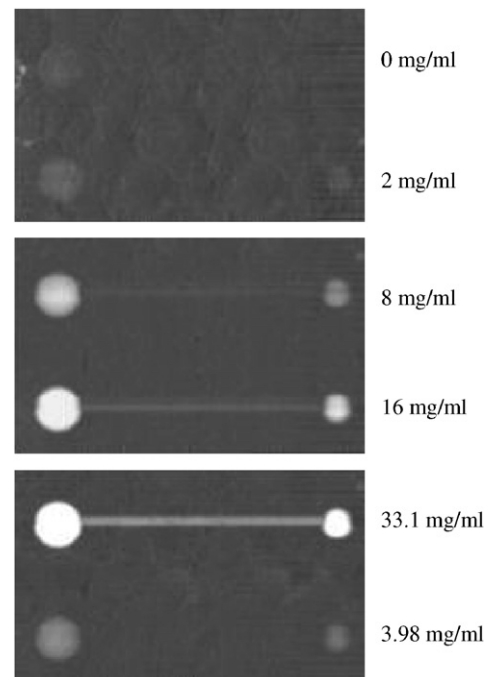


Fig. 2. KESM technique with monochromatic X-rays. Final images obtained from initial images acquired at 32.5 and 33.9 keV for a total exposure of 1.84 mGy corresponding to a MGD of 1.73 mGy.

phantom above and below the contrast medium K-edge energy (33.17 keV) have been acquired at $E_- = 32.5$ keV and $E_+ = 33.9$ keV, respectively.

For the TSM technique, images of the phantom with energy above the K-edge (33.9 keV), have been acquired before and after contrast medium administration. For each technique images corresponding to three different mean glandular dose levels have been acquired. Mean glandular dose values have been obtained by measuring the incident air kerma and by applying the incident air kerma to mean glandular dose conversion factors published by Moeckly et al. [4].

2.3.2. Image acquisition with a clinical digital system

The clinical digital system used is the Senographe 2000D (GE Medical Systems, Milwaukee, WI) that integrates a digital detector composed of a 100 μ m thick thallium-doped CsI scintillator, an amorphous silicon photodiode array for indirect X-ray detection and special purpose readout electronics. The KESM technique has been applied

by using spectra chosen in accordance with Lewin [6], who applied the technique in a clinical investigation and studied the spectra optimization. In particular, the image below the iodine K-edge has been acquired at 30 kV_p with a molybdenum target-molybdenum filter combination and 140 mAs. The image above the K-edge has been acquired at 46 kV_p with a rhodium target-rhodium filter combination, a further filtration of 6 mm of aluminium and 200 mAs. This spectrum has also been used for the TSM technique.

3. Results and discussion

3.1. KESM and TSM techniques with monochromatic X-rays

Fig. 2 reports final images obtained from the application of the KESM technique for details filled with iodine concentration of 8 and 16.1 mg/ml, as well as 0, 2, 33.1 and 3.98 mg/ml. Fig. 3 shows results of the image CNR

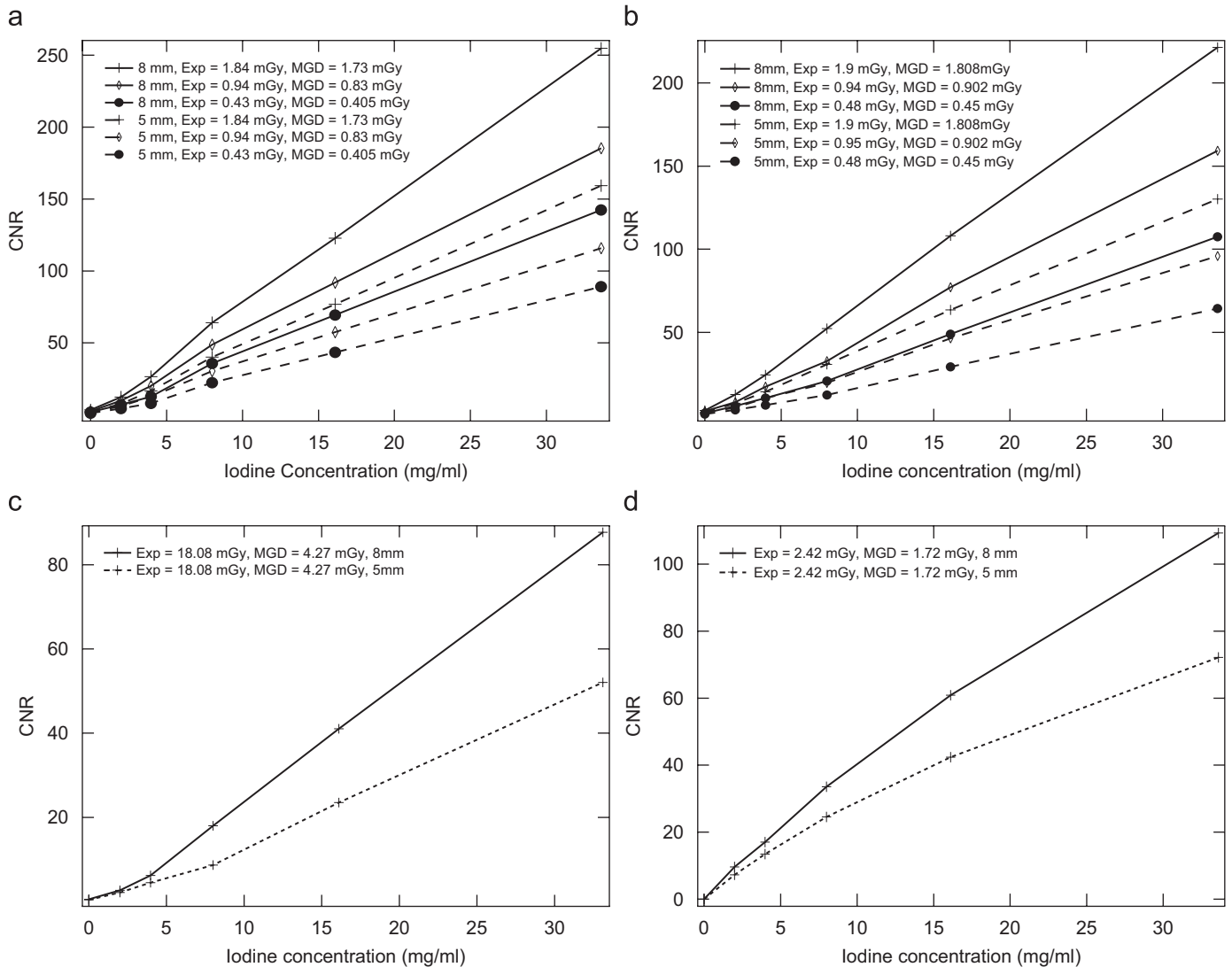


Fig. 3. Results of KESM (a) and TSM (b) with monochromatic beams, KESM (c) and TSM (d) with a clinical digital system: CNR as a function of the iodine concentration.

as a function of the iodine concentration for three different exposure conditions and two detail diameters, for KESM and TSM, respectively. In both cases there is a linear relation between CNR and iodine concentration.

3.2. KESM and TSM techniques with a clinical digital system

Fig. 3 shows results of the image CNR as a function of the iodine concentration for both techniques.

For the TSM technique the trend is not perfectly linear for any of the cavity sizes and this behavior can be explained as in the following. As the iodine concentration, on the post-contrast image, increases, the mean energy of the beam impinging on the detector in correspondence of the cavity, increases due to the beam hardening effect. This means that the signal of the cavity decreases according to the difference in detector absorption at the different mean energies before and after iodine administration.

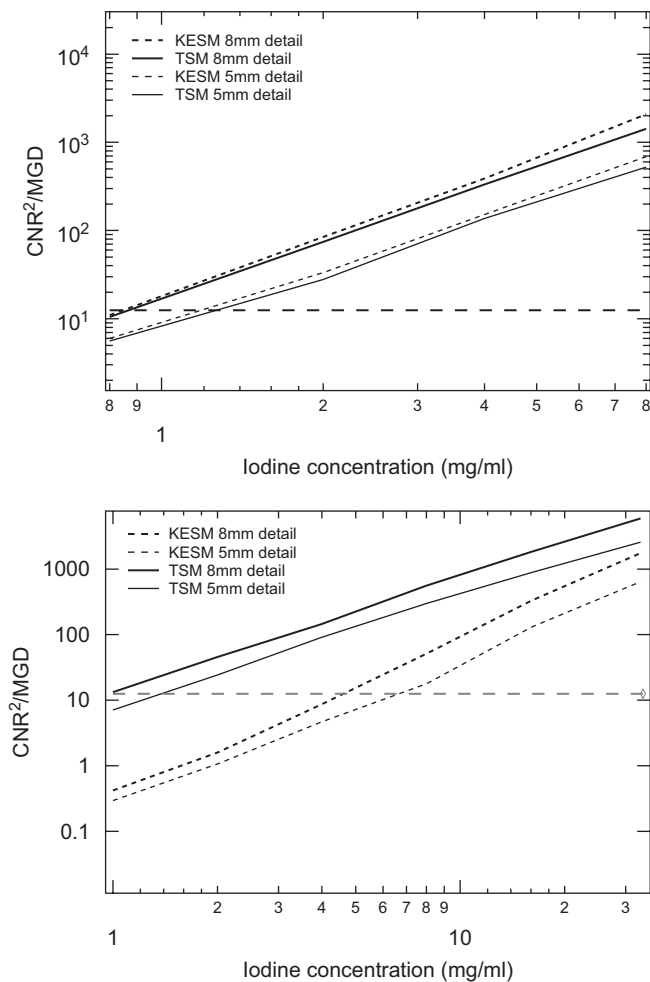


Fig. 4. CNR^2/MGD as a function of the iodine concentrations for monochromatic X-rays (top) and a clinical digital system (bottom). The dashed line represents the value 12.5 corresponding to $\text{CNR} = 5$ and $\text{MGD} = 2 \text{ mGy}$.

Table 1

Minimum concentration of iodine required to visualize cavities with $\text{CNR} = 5$ and $\text{MGD} = 2 \text{ mGy}$

<i>KESM technique</i>		
Source (mm)	8	5
Sync. Rad. (mg/ml)	0.90	1.34
Clinic. system (mg/ml)	4.13	5.75
<i>TSM technique</i>		
Source (mm)	8	5
Sync. Rad. (mg/ml)	0.84	1.31
Clinic. system (mg/ml)	1.01	1.57

3.3. Comparison of results obtained with polychromatic and monochromatic beams

The CNR^2/MGD as a function of iodine concentration for both techniques and both sources is reported in Fig. 4. From these graphs the minimum iodine concentration needed to obtain a $\text{CNR} = 5$ and $\text{MGD} = 2 \text{ mGy}$ have been determined. Results are reported in Table 1. The minimum concentrations required for applying dual-energy techniques with the clinical system are higher than those estimated for the application of synchrotron radiation source. In particular, the KESM technique with synchrotron radiation needs a concentration about 80% less than that estimated for the conventional system. This difference is not so high for the TSM technique, where only a concentration reduction of about 20% is needed.

These results are a consequences of the intrinsic differences of the two sources. The large difference between the two systems for the KESM technique is due to the advantages offered by the synchrotron radiation: the better energy separation achievable and the reduction of the absorbed dose due to the elimination of lower energy X-rays. In fact, conventional beams consist of a continuous bremsstrahlung component in which X-rays with high energy produce scattered radiation in the object, degrading the object contrast, and X-rays with low energy produce an undesired absorbed dose. There is still a difference between the two systems using the TSM, which is due to the less scattered radiation obtainable with collimating system, which improve the image contrast. At a parity of X-rays sources, the KESM and TSM techniques are comparable if applied with a synchrotron radiation source. The TSM technique is preferable if a conventional digital system is used, but if applied to structures in motion requires image-matching technique in order to minimize the effect of motion between the images acquisition.

References

- [1] M.N. Linver, Radiology 184 (1992) 39.
- [2] L.A. Lehmann, R.E. Alvarez, A. Macovski, W.R. Brody, Med. Phys. 8 (1981) 659.
- [3] M. Skarpathiotakis, M.J. Yaffe, A.K. Bloomquist, Med. Phys. 29 (2002) 2419.
- [4] R. Moeckly, F.R. Verdun, S. Fiedler, et al., Phys. Med. Biol. 35 (2000) 3509.
- [5] H. Elleaume, et al., Nucl. Instr. and Meth. A 428 (1999) 513.
- [6] J.M. Lewin, P.K. Isaacs, V. Vance, F.J. Larke, Radiology 229 (2003) 261.